

8. Chesnavich W. J.; Bowers, M. T. *Prog. React. Kinet.* **1982**, *11*, 137.
9. Malinovich, Y.; Arakawa, R.; Haase, G.; Lifshitz, C. J. *Phys. Chem.* **1985**, *89*, 2253.
10. Jarrold, M. F.; Wagner-Redeker, W.; Illies, A. J.; Kirchner, N. J.; Bowers, M. T. *Int. J. Mass Spectrom. Ion Processes* **1984**, *58*, 63.
11. Bunn, T. L.; Bowers, M. T. *J. Phys. Chem.* **1988**, *92*, 1813.
12. Snodgrass, J. T.; Dunbar, R. C.; Bowers, M. T. *J. Phys. Chem.* **1990**, *94*, 3648.
13. Cooks, R. G.; Beynon, J. H.; Caprioli, R. M.; Lester, G. R. *Metastable Ions*; Elsevier: Amsterdam, 1973; p 104.
14. Levsen, K. *Fundamental Aspects of Organic Mass Spectrometry*; Verlag Chemie: Weinheim, 1978; p 134.
15. Marcus, R. A. *J. Chem. Phys.* **1975**, *62*, 1372.
16. Worry, G.; Marcus, R. A. *J. Chem. Phys.* **1977**, *67*, 1636.
17. Parson, J. M.; Lee, Y. T. *J. Chem. Phys.* **1972**, *56*, 4658.
18. Yeh, I. C.; Kim, Y. H.; Kim, M. S. *Chem. Phys. Lett.* **1993**, *207*, 487.
19. Sloan, J. J. *J. Phys. Chem.* **1988**, *92*, 18.
20. Yeh, I. C., Kim, M. S. *Rapid Commun. Mass Spectrom.* **1992**, *6*, 115.
21. Yeh, I. C.; Kim, M. S. *Rapid Commun. Mass Spectrom.* **1992**, *6*, 293.
22. Kim, Y. H.; Kim, M. S. *Rapid Commun. Mass Spectrom.* **1991**, *5*, 25.
23. Brigham, E. O. *The Fast Fourier Transform and Its Applications*; Prentice-Hall: London, 1988; p 204, p 345.
24. Robinson, P. J.; Holbrook, K. A. *Unimolecular Reactions*; Wiley-Interscience: New York, 1972; p 64.
25. Forst, W. *Theory of Unimolecular Reactions*; Academic Press: New York, 1973; p 28.
26. Chesnavich, W. J.; Bowers, M. T. *J. Phys. Chem.* **1979**, *83*, 900.
27. Reinke, D.; Kraessig, R.; Baumgärtel, H. *Z. Naturforsch.* **1973**, *28a*, 1021.
28. Lias, S. G.; Bartmess, J. E.; Liebman, J. F.; Holmes, J. L.; Levin R. D.; Mallard, W. G. *J. Phys. Chem. Ref. Data* **17 Suppl. 1**, **1988**, *81*, 83, 604.
29. Traeger, J. C.; McLoughlin, R. G. *J. Am. Chem. Soc.* **1981**, *103*, 3647.
30. Grice, M. E.; Song, K.; Chesnavich, W. J. *J. Phys. Chem.* **1986**, *90*, 3503.
31. Smith, D. C.; Nielsen, J. R.; Claassen, H. H. *J. Chem. Phys.* **1950**, *18*, 326.
32. Hunt, G. R.; Wilson, M. K. *J. Chem. Phys.* **1961**, *34*, 1301.
33. Herzberg, G. *Molecular Spectra and Molecular Structure, I. Spectra of Diatomic Molecules*; D. Van Nostrand Company: 2nd ed; New York, p 536.
34. Lafferty, W. J.; Sattler, J. P.; Worchesky, T. L.; Ritter, K. J. *J. Mol. Spectrosc.* **1981**, *87*, 416.
35. Jones, H.; Rudolph, H. D. *Z. Naturforsch.* **1979**, *34a*, 340.
36. Hirschfelder, J. O.; Curtiss, C. F.; Bird, R. B. *Molecular Theory of Gases and Liquids*; John Wiley & Sons: New York, 1954; p 950.

The Crystal and Molecular Structure of Sodium Magnesium Tris(oxalato)Chromate(III) Decahydrate, $\text{NaMg}[\text{Cr}(\text{ox})_3] \cdot 10\text{H}_2\text{O}$

Jung-Sun Suh, Jung-Yup Shin, Cheonho Yoon, Kyu-Wang Lee
Il-Hwan Suh*, Jin-Ho Lee*, Bo-Young Ryu*, and Sung-Su Lim*

Department of Chemistry, Myongji University Yongin, Kyonggi-do 449-728

**Department of Physics, Chungnam National University, Taejon 305-764*

Received November 2, 1993

$\text{NaMg}[\text{Cr}(\text{C}_2\text{O}_4)_3] \cdot 10\text{H}_2\text{O}$ crystallizes in the trigonal space group $\text{P}\bar{3}\text{c}1$, with $a=b=16.969(3)$, $c=12.521(3)$ Å, $\alpha=\beta=90^\circ$, $\gamma=120^\circ$, $\rho=1.734$ g cm⁻³, $\mu=6.46$ cm⁻¹, $Z=6$. Intensities for 1062 unique reflections were measured on a four-circle diffractometer with Mo K α radiation ($\lambda=0.71069$ Å). The structure was solved by direct methods and refined to a final ωR value of 0.084. X-ray crystal structure showed that magnesium ion appears to be occupied over two sites with the occupancy ratio of 2 : 1. The crystal possesses 10 water molecules instead of previously estimated 9 water molecules.

Introduction

Even though the magnetic and electronic properties of $[\text{Cr}(\text{ox})_3]^{3-}$ [$\text{ox}=(\text{C}_2\text{O}_4)^{2-}$] have been extensively studied under the guidelines of conventional ligand field theory, the results are not always in agreement.¹⁻³ The type of space group has been controversially discussed for the interpretation of EPR and PMR results.⁴ Band assignments in the sharp lines

arising from t_{2g}^3 intraconfigurational transition are still controversial.

Mortensen reported 20 cm⁻¹ splitting of 2E_g line in NaMg salt,² while Coleman observed large variance of 2E_g splittings (from 2 to 115 cm⁻¹) which have been attributed to the degree of hydration and the effects of the counter ion in a molecule.⁵ Recently Schönherr *et al.* assigned the 2E_g lines split by 2-3 cm⁻¹ which was rationalized by the angular over-

lap model calculation on the basis of D_3 symmetry with variation of angular geometry.⁶ Hoggard suggested that the anisotropic π -bonding could alter the sharp line position significantly and may result in a very large 2E_g splittings.⁷

Since the splittings of sharp lines are very sensitive to the metal-ligand geometry, the knowledge of crystal and molecular structure is essential for the detailed analyses of electronic and magnetic properties. The available structural data of this complex up to now, however, are very limited. We give here the result of an accurate three-dimensional single crystal X-ray analysis of the structure of $\text{NaMg}[\text{Cr}(\text{ox})_3] \cdot 10\text{H}_2\text{O}$

Experimental

Sodium tris(oxalato)chromate(III), $\text{Na}_3[\text{Cr}(\text{ox})_3] \cdot 3\text{H}_2\text{O}$ was prepared by standard method.⁸ Twice crystallized $\text{Na}_3[\text{Cr}(\text{ox})_3] \cdot 3\text{H}_2\text{O}$ (4.39 g) and $\text{MgCl}_2 \cdot 6\text{H}_2\text{O}$ (2.03 g) were dissolved in water and recrystallized by slow evaporation in the dark. Dark blue hexagonal crystals were obtained.⁹

The Laue group of the crystal was confirmed by X-ray photography.¹⁰ A crystal of approximate dimensions of $0.4 \times 0.5 \times 0.3$ mm was mounted and aligned on an Enraf-Nonius CAD-4 diffractometer. The accurate cell parameters were refined from setting angles of 25 reflections with $11.521^\circ < \theta < 13.975^\circ$. The systematic absences of $hkl : l = 2n$ and $00l : l = 2n$ showed two possible space groups $P\bar{3}c1$ and $P3c1$. The space group, $P\bar{3}c1$, was confirmed after the elucidation of the crystal structure. The 1062 independent reflections in the range of $0 \leq h \leq 16$, $0 \leq k \leq 16$, $0 \leq l \leq 14$ for an asymmetric unit¹¹ were collected using graphite-monochromated Mo K α radiation and $\omega/2\theta$ scan mode, ω -scan angle = $(0.65 + 0.34 \tan \theta)^\circ$, $\theta_{\text{max}} = 24^\circ$. All data were converted to E_o values following correction for L-P factors. The four heavy atoms were located by using direct method (SHELX86)¹² and all non-hydrogen atoms were found on subsequent difference Fourier maps. The structure was refined by full-matrix least squares with SHELX76¹³ and function minimized was $\Sigma w(|F_o| - |F_c|)^2$ with unit weights.

The positions of Cr, Na, Mg and Mg^* atoms were assigned according to their electronic densities and later on they were confirmed by interatomic bond lengths and angles. As the heavy atoms Cr, Na, Mg and Mg^* are on the special positions, they were refined with fixed occupancy factors of 1/2, 1/2, 1/6 and 1/3 respectively and with $u_{22} = 2u_{12}$, $2u_{23} = u_{13}$ for Cr and Na, $u_{11} = u_{22} = 2u_{12}$, $u_{13} = u_{23}$ for Mg and Mg^* atoms.¹⁴ Number of parameters refined was 138. A final difference Fourier synthesis showed a number of small peaks in the vicinity of the heavy atoms. Final reliability factors were $R = 0.084$ with average $\Delta/\sigma = 0.0026$, $\Delta\rho_{\text{max}}/\Delta\rho_{\text{min}} = 0.69 / -0.96e \text{ \AA}^{-3}$ in the final $\Delta\rho$ map, and $S = 4.56$. Final positional parameters, occupancy factor and U_{eq} for non-hydrogen atoms are given in Table 1. All computations were carried out using the MICROVAX/3400 computer.

Results and Discussion

As shown in Table 1, Cr and Na atoms occupy special positions with 2-fold symmetry with their occupancy factors of 1/2. The magnesium ion occupies over two sites in such a way that one third of Mg is located at (0, 0, 1/4) with

Table 1. Final atomic coordinate ($\times 10^4$), occupancy factors ($\text{\AA} \times 10^3$) and equivalent isotropic thermal ($\text{\AA}^2 \times 10^4$) parameters with e.s.d.'s in parentheses

Atom	x	y	z	Occup.	U_{eq}
Cr	10000(0)	6599(1)	2500(0)	1/2	19
Mg	10000(0)	10000(0)	-2500(0)	1/6	27
Mg^*	6667(0)	3333(0)	2572(0)	1/3	10
Na	6754(6)	6754(0)	2500(0)	1/2	38
O(1)	8858(5)	6089(5)	3328(6)	1	28
O(2)	9406(5)	7118(5)	1624(6)	1	29
O(3)	10476(6)	5959(5)	3377(6)	1	27
O(4)	8149(5)	7223(6)	1588(7)	1	36
O(5)	7618(6)	6242(6)	3455(7)	1	36
O(6)	10585(6)	4705(5)	3372(7)	1	31
O(7)	9433(12)	8864(13)	-1538(13)	1	211
O(8)	8402(12)	8310(12)	-0047(15)	1	130
O(9)	7492(5)	3043(5)	1586(6)	1	26
O(10)	6379(5)	2222(5)	3500(6)	1	23
O(11)	6711(5)	1754(4)	8(6)	1	20
C(1)	8629(8)	6951(8)	1974(11)	1	25
C(2)	8308(8)	6359(9)	3021(11)	1	27
C(3)	10314(8)	5185(7)	2988(10)	1	22

Table 2. The calculation of the number of atoms in a molecule

Atom	Occupancy factor	No. of symmetry	No. of atom
Cr	1/2	2	1
Mg(1)	1/6	2	1/3
Mg(2)	1/3	2	2/3
Na	1/2	2	1
O(6 atoms)	1	2	12
C(3 atoms)	1	2	6
O(5 water molecules)	1	2	10

2-fold and 3-fold symmetries, and two-third of it, Mg^* , is located at (2/3, 1/3, 0.2573) with a 3-fold symmetry. Therefore the occupancy factors of Mg and Mg^* atoms are 1/6 and 1/3, respectively. Since in a molecule itself there is a 2-fold symmetry along (110) at the site of $z = 1/4$, the half molecule of this compound is in the asymmetric unit and the chemical formula of the molecule is $\text{NaMg}[\text{Cr}(\text{C}_2\text{O}_4)_3] \cdot 10\text{H}_2\text{O}$ as shown in Table 2.

The main bond lengths and angles in $\text{Cr}(\text{ox})_3^{3-}$ unit and the environments of Na^+ , Mg^{2+} ions and water molecules are characterized by their nearest neighbor contacts in Table 3 and 4. The perspective drawing of $\text{Cr}(\text{ox})_3^{3-}$ anion with atomic numbering scheme and the crystal packing of $\text{NaMg}[\text{Cr}(\text{ox})_3] \cdot 10\text{H}_2\text{O}$ are shown in Figure 1 and 2 respectively.

The X-ray structural analysis reveals the composition of the complex as decahydrate, $\text{NaMg}[\text{Cr}(\text{ox})_3] \cdot 10\text{H}_2\text{O}$. This has been reported as nonhydrate without the inclusion of analytical data, but presumably by elemental analysis.^{1,2,8,9} The similarity in elemental percentage between nona and decahydrate could have led to nonhydrate formula.

Table 3. Interatomic distances (Å) and e.s.d.'s in parentheses

Cr-O(1)	1.977(8)	Cr-O(2)	1.970(8)	Cr-O(3)	1.976(8)
Cr-O(1 ^a)	1.977	Cr-O(2 ^a)	1.970	Cr-O(3 ^a)	1.976
Mg-O(7)	2.062(13)	Mg-O(7 ^a)	2.062	Mg-O(7 ^b)	2.062
Mg-O(7 ^c)	2.062	Mg-O(7 ^b)	2.062	Mg-O(7 ^c)	2.062
Mg [*] -O(9)	2.101(10)	Mg [*] -O(9 ^b)	2.103	Mg [*] -O(9 ^c)	2.103
Mg [*] -O(10)	2.054(10)	Mg [*] -O(10 ^b)	2.055	Mg [*] -O(10 ^c)	2.055
Na-O(4)	2.378(12)	Na-O(4 ^a)	2.382	Na-O(5)	2.372(13)
Na-O(5 ^a)	2.369	Na-O(6 ^b)	2.416	Na-O(6 ^c)	2.417
O(1)-C(2)	1.287(13)	O(2)-C(1)	1.280(14)	O(3)-C(3)	1.294(13)
O(4)-C(1)	1.221(14)	O(5)-C(2)	1.217(14)	O(6)-C(3)	1.214(12)
C(1)-C(2)	1.571(16)	C(3)-C(3 ^a)	1.536(27)		

key to the symmetry operations:

(a) 2-X, 1+Y-X, 1.5-Z	(b) 1-Y, X-Y, Z	(c) Y, X, 1.5-Z
(d) 1+Y-X, 1-X, Z	(e) 1-Y, -1+X-Y, Z	(f) 2-X+Y, 1-X, Z
(g) 1+Y, -1+X, 1.5-Z	(h) 2-X, 1-X+Y, 1.5-Z	(i) X-Y, -Y, 1.5-Z
(j) X-Y, 1-Y, 1.5-Z		

Table 4. Selected interatomic angles (°) with e.s.d.'s in parentheses

O(1)-Cr-O(2)	83.1(3)	O(1)-Cr-O(3)	92.7(3)	O(1)-Cr-O(1 ^a)	174.0(5)
O(1)-Cr-O(2 ^a)	92.7	O(1)-Cr-O(3 ^a)	91.5	O(2)-Cr-O(1 ^a)	92.7
O(2)-Cr-O(2 ^a)	90.7(5)	O(2)-Cr-O(3)	174.4	O(2)-Cr-O(3 ^a)	93.5
O(3)-Cr-O(1 ^a)	91.5	O(3)-Cr-O(1 ^a)	93.5	O(3)-Cr-O(3 ^a)	82.2(5)
O(1 ^a)-Cr-O(2 ^a)	82.9	O(1 ^a)-Cr-O(3 ^a)	93.2	O(2 ^a)-Cr-O(3 ^a)	174.4
O(7)-Mg-O(7 ^a)	89.2(6)	O(7)-Mg-O(7 ^b)	179.7	O(7)-Mg-O(7 ^b)	91.6
O(7)-Mg-O(7 ^c)	90.7(12)	O(7 ^a)-Mg-O(7 ^c)	89.2	O(7 ^a)-Mg-O(7 ^c)	90.9(12)
O(7 ^a)-Mg-O(7 ^b)	179.7	O(7 ^b)-Mg-O(7 ^b)	90.9	O(7)-Mg-O(7 ^a)	89.2(6)
O(9)-Mg [*] -O(10)	89.9(3)	O(9)-Mg [*] -O(10 ^b)	90.2	O(9 ^b)-Mg [*] -O(10 ^b)	88.4
O(4)-Na-O(4 ^b)	96.7(7)	O(4)-Na-O(5)	70.6(4)	O(4)-Na-O(5 ^a)	99.2
O(4)-Na-O(6)	164.7	O(4 ^b)-Na-O(5 ^b)	70.6	O(4 ^a)-Na-O(6 ^b)	97.1
O(5)-Na-O(4 ^a)	99.2	O(5)-Na-O(5 ^b)	165.3	O(5)-Na-O(6 ^a)	100.6
O(5 ^a)-Na-O(6 ^b)	91.6	O(6)-Na ^a -O(6)	70.1	Cr-O(1)-C(2)	114.5(7)
Cr-O(2)-C(1)	114.3(7)	Cr-O(3)-C(3)	114.1(7)	Na-O(4)-C(1)	115.2(8)
Na-O(5)-C(2)	116.0(8)	O(1 ^b)-O(10)-O(11 ^b)	118.1	Na ^a -O(6)-C(3)	115.4
O(9)-O(11)-O(10 ^b)	113.5	O(2)-C(1)-O(4)	126.2(11)	O(2)-C(1)-C(2)	114.6(10)
O(4)-C(1)-C(2)	119.2(11)	O(1)-C(2)-C(1)	113.2(10)	O(5)-C(2)-C(1)	118.4(11)
O(3)-C(3)-C(3 ^a)	114.4	O(3)-C(3)-O(6)	124.8(12)	O(6)-C(3)-C(3 ^a)	121.9

key to the symmetry operations:

(a) 2-X, 1+Y-X, 1.5-Z	(b) 1-Y, X-Y, Z	(c) Y, X, 1.5-Z
(d) 1+Y-X, 1-X, Z	(e) 1-Y, -1+X-Y, Z	(f) 2+Y-X, 1-X, Z
(g) 1+Y, -1+X, 1.5-Z	(h) 2-X, 1+Y-X, 1.5-Z	(i) X-Y, -Y, 0.5-Z
(j) 1+Y-X, Y, 0.5-Z	(k) 1+Y-X, Y, -0.5+Z	

The structure of $\text{Cr}(\text{ox})_3^{3-}$ anion in the complex is very similar to that of $\text{K}_3[\text{Cr}(\text{ox})_3] \cdot 3\text{H}_2\text{O}$, structure determined by Talyor.¹⁵ The average bond length of Cr-O is 1.977 Å. The octahedron around the Cr atom is distorted by up to 16.0° from the ideal value of 90 and 180°, and the oxalate ligands are nearly planar within 0.1291(10) Å deviation from the plane. In oxalate ligands, inner C-O bonds (Avg. 1.288 Å), where the oxygen is coordinated to the Cr^{3+} ion are longer than the outer C-O bonds (Avg. 1.216 Å) which may represent the double bond character of outer C-O bond. The average bond length of C-C is 1.588 Å.

The crystallographic environments of Na^+ and Mg^{2+} ions

are very peculiar. Na^+ ion is attached to oxygen atoms of oxalate anion while Mg^{2+} ion is surrounded by oxygen atoms of water molecules, presumably through the electrostatic attraction. Na^+ ions are attached to outer oxalate oxygen atoms (O4, O5, O6 and three other oxygens generated by 2-fold symmetry) and three oxalate groups are surrounding Cr^{3+} , Na^+ ions alternatively with the same z-coordinate by 1/4, so these form an infinite layer parallel to (001) plane with interlayer distance of 6.26 Å (Figure 2). The Na-O distances range from 2.371 to 2.415 Å with mean value of 2.388 Å. This agrees well with sum of effective ionic radii of Na^+ (1.16 Å) and O^{2-} (1.21 Å) and with the Na-O distance of sodium D-tartrate

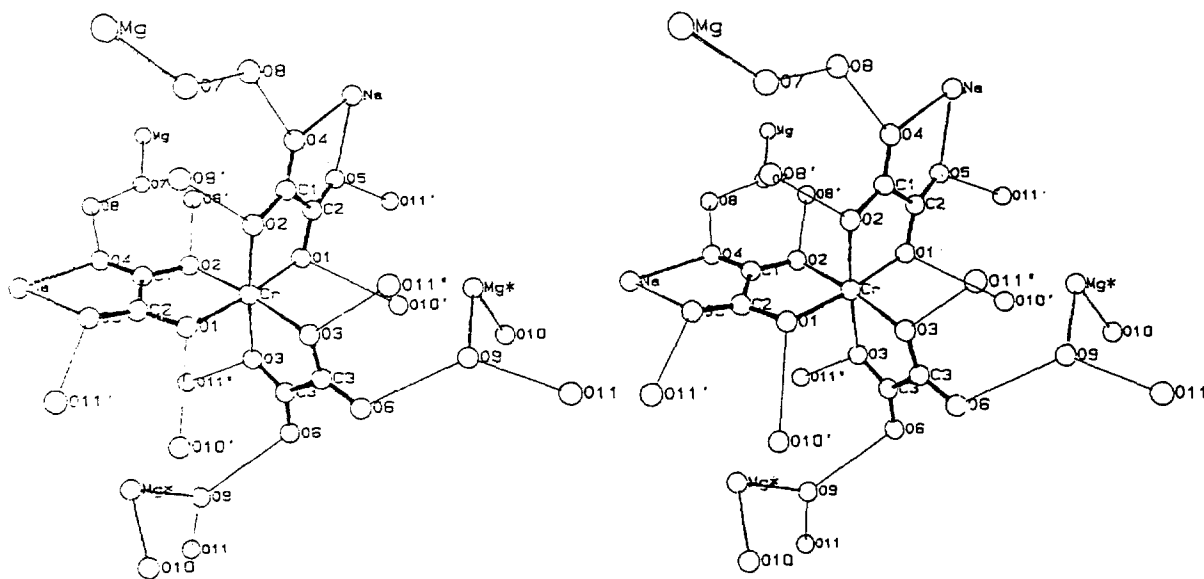


Figure 1. Molecular structure and atomic labelling scheme. The asymmetric unit corresponds to one-half of the molecule, the other half being generated by the crystallographic two fold axis.

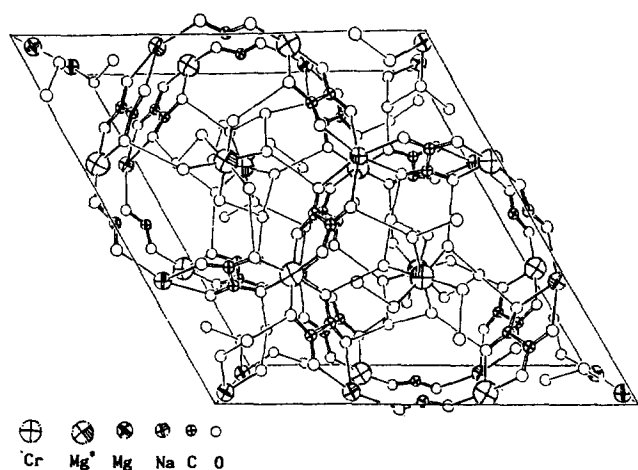


Figure 2. A diagram of a unit-cell packing for the molecule: origin, lower left; a-axis, horizontal; b-axis, vertical.

dihydrate.¹⁶

Two different Mg^{2+} sites in this complex are manifested from difference Fourier map. Oxygen atoms of crystalline water around the Mg and Mg^* atoms form the different geometry in such a way that Mg interact with O(7) and symmetry-related five other O(7) atoms and Mg^* interact with O(9), O(10) and the symmetry-related four other themselves. This produces octahedral environment for the Mg^{2+} ions (Figure 3 and 4). The Mg-O distances vary from 2.053 to 2.101 Å with mean value of 2.068 Å as summarized in Table 3 and 4. This is in good agreement with 2.074 Å found in $[Mg(H_2O)_6]^{2+}$ ion.¹⁷ The other oxygens from crystalline waters (O(8), O(9)) are located in between Mg and Mg^* ions, and they are associated with other oxygen atoms of oxalate anions and of water molecules, probably through hydrogen bonding. Though the definite proof for hydrogen bonding is lacking since the hydrogen atoms of the water molecules could not be located, one may take the evidence of hydrogen bonding if O-O dista-

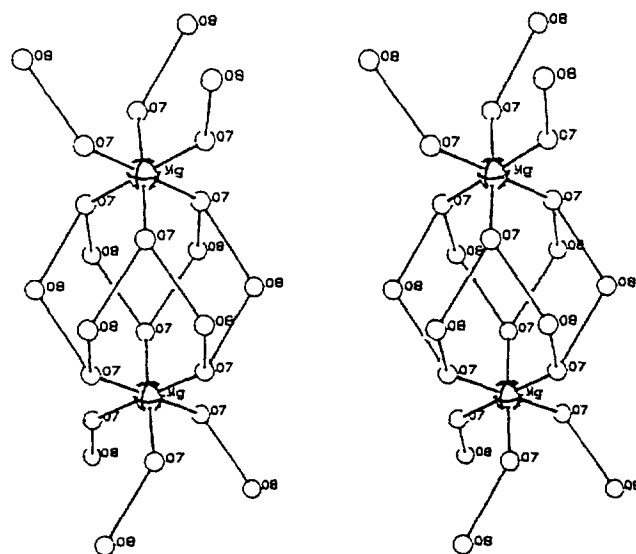


Figure 3. A stereoview of the environment of Mg atom.

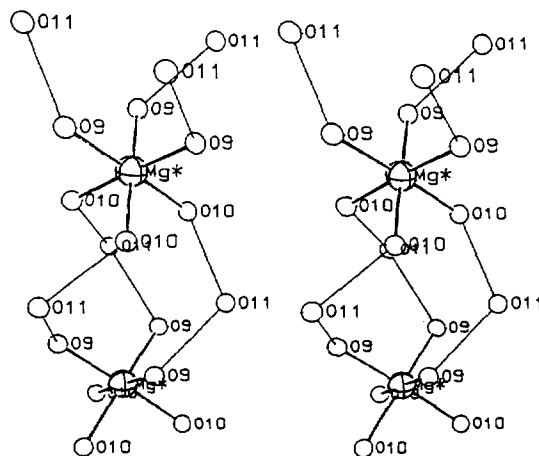


Figure 4. A stereoview of the environment of Mg^* atom.

nce less than 3 Å which is sum of the van der Waals radius of oxygen. These hydrogen bonds formed through water molecules interconnect the two parallel layers of sodium tris (oxalato) chromate unit separated by $c/2$ and may stabilize the molecular packing.

These two Mg^{2+} ions will create two different ligand field environment for the $Cr(ox)_3^{3-}$ and may cause the small ($2-3\text{ cm}^{-1}$) splitting in optical spectrum. One may suggest the possibility of this splitting as zero field splitting. However, EPR study suggested the magnitude of zero field splitting as 0.9 cm^{-1} . Mortensen suggested that this optical splitting is due to exchange interaction between separate $Cr(ox)_3^{3-}$ ions.² But it is very unlikely since the closest Cr-Cr separation is determined as 8.282 Å and the same splitting is observed in 1-5% $Cr(ox)_3^{3-}$ doped in NaMg salt of $Al(ox)_3^{3-}$ complex where the separation of Cr-Cr is even expected to be larger.

Acknowledgement. This work was supported by Non-directed Research Fund, Korea Research Foundation. I.-H. Suh thanks the Korean Science and Engineering Foundation for the support.

References

1. Condrate, R. A.; Forster, L. S. O. *J. Mol. Spectros.* **1967**,

24, 490.

2. Mortensen, O. S. *J. Chem. Phys.* **1967**, 47, 4215.

3. Coleman, W. F. Coleman, *J. Lumin.* **1975**, 10, 163.

4. Berheim, R. A.; Reichenbecher, E. F. *J. Chem. Phys.* **1969**, 51, 996.

5. Coleman, W. F. *J. Lumin.* **1980**, 22, 17.

6. Schönherr, T.; Spanier, J.; Schmidtke, H.-H. *J. Phys. Chem.* **1989**, 93, 5969.

7. Hoggard, P. E.; *Coord. Chem. Rev.* **1986**, 70, 85.

8. Bailar, J. C.; Jones, E. M. *Inorg. Synthesis.* **1939**, 1, 35.

9. Gmelines handbuch der Anorganische Chemie, *System 52 (Chromium)*, Teil B, **1962**, 791.

10. Suh, I. H.; Choo, G. H.; Lee, J. H.; Lim, S. S.; Ryu, B. *Y. Chungnam J. Sci.* **1992**, 19, 87.

11. Suh, I. H.; Kim, K. J.; Choo, G. H.; Lee, J. H.; Choh, S. H.; Kim, M. J. *Acta Cryst.* **1993**, A49, 369.

12. Sheldrick, G. M. SHELX-86, Univ. Goettingen, Federal Republic of Germany.

13. Sheldrick, G. M. SHELX-76, *A program for Crystal Structure Determination*, Univ. of Cambridge, England **1976**.

14. Peterse, W. J. A. M.; Plam, J. H. *Acta Cryst.* **1966**, 20, 147.

15. Taylor, D. *Aust. J. Chem.* **1978**, 31, 1455.

16. Ambady, G. K.; Kartha, G. *Acta Cryst.* **1968**, B24, 1540.

17. Johnson, C. K. *Acta Cryst.* **1965**, 18, 1004.

Time-resolved UV Fluorescence Spectroscopy of Aorta and its Related Chromophores, Collagen and Elastin, Using 320 nm Excitation

Young D. Park

Department of Chemistry Ajou University, Suwon 441-749

Received December 24, 1993

Fluorescence time decay of human aorta has been measured at 380, 440, 480 nm using 320 nm excitation and time-correlated single photon counting technique. Fluorescence decay was found to be nonexponential at all emission frequencies. The normal and diseased sample showed significantly different fluorescence behaviors at 380 nm while this time decay difference was decreased in the fluorescence at 440 and 480 nms. The decay data were multiexponential and were analyzed with two exponential decay constants. The fluorescence decays were compared with and analyzed in terms of collagen and elastin.

Introduction

Laser-induced fluorescence (LIF) spectroscopy has proved to be one of the most sensitive detection methods and has become a powerful tool in the field of analytical chemistry. LIF spectroscopy has been widely used in biology and medicine and more recently in the characterization of human tissue.¹⁻⁴ The study of arterial wall spectroscopy, in particular, has drawn considerable interest because atherosclerosis account for a large proportion of heart attacks and cases of ischemic heart disease⁵. Atherosclerosis also accounts for many strokes, numerous instances of peripheral disease, most aneurysms of the lower abdominal aorta, which can rup-

ture and cause sudden fatal hemorrhage⁶. Laser induced fluorescence has great potential for arterial wall diagnosis due to its sensitivity, and its ability to be monitored remotely using optical fiber probe. Since fluorescence emission is affected by the fluorophors constitution and their surrounding environments, normal and diseased plaque tissue are expected to yield different fluorescence behavior both in frequency and time domain. In this paper, we would like to focus our discussion on the time resolved study of aorta fluorescence spectroscopy.

Aorta is a large elastic artery and is made of three major microscopic layers: the intima, the media, and the adventitia⁶. These layers are separated by elastic sheets. The intima is